

# MAPPING LATERAL VARIATIONS IN UPPER MANTLE ATTENUATION USING STACKS OF P AND PP SPECTRA

Linda Warren and Peter M. Shearer

Institute of Geophysics and Planetary Physics  
Scripps Institution of Oceanography  
University of California, San Diego

Sponsored by the National Science Foundation  
Grant EAR-9909267

## **ABSTRACT**

Using seismograms from globally-distributed, shallow earthquakes between 1988 and 1998, we compute over 30,000 spectra of  $P$  arrivals from epicentral distances of  $40^\circ$  to  $80^\circ$  and  $PP$  arrivals from  $80^\circ$  to  $160^\circ$ . We correct each spectrum for the instrument response, an  $\omega^{-2.15}$  source model, and a one-dimensional  $Q_\alpha$  model (Warren and Shearer, 2000). Next, we stack the logarithms of the  $P$  and  $PP$  spectra in bins of similar source-receiver range. The stacked log-spectra appear stable between about 0.16 and 0.86 Hz, with noise and/or bias affecting the results at higher frequencies. Since we have multiple sources for each receiver and multiple receivers for each source, we can measure the attenuation beneath each source and receiver by stacking the appropriate  $P$  log-spectra. We then correct the  $PP$  log-spectra for the appropriate source and receiver-side terms. Since lower mantle attenuation is small, the residual  $PP$  log-spectrum approximates attenuation in the upper mantle near the  $PP$  bounce point. Using this approach, we produce maps of global variations in average  $P$ -wave upper mantle attenuation. These results generally correlate with surface tectonics and previously published  $Q$  models. Continents are usually less attenuating than the global average, whereas oceanic regions are more attenuating. Notable exceptions to this pattern include southern Africa (more attenuating than average) and the southwest Pacific (less attenuating than average).

**Key Words:** Seismic Attenuation, Upper Mantle Structure

## **OBJECTIVE**

The objective of this research is to resolve variations in upper mantle  $P$ -wave attenuation by analyzing short-period  $P$  and  $PP$  spectra. Results of this research will help to establish detection levels for small events and calibrate magnitude versus yield relationships for explosions.

## **RESEARCH ACCOMPLISHED**

### *Data and Methods*

We select our seismograms from the IRIS FARM database between 1988 and 1998. We search the database, which we have filtered and resampled at 5 Hz, for all  $P$  arrivals at epicentral distances between  $40^\circ$  and  $80^\circ$  and all  $PP$  arrivals between  $80^\circ$  and  $160^\circ$  (i.e., twice the  $P$  range interval) from shallow ( $<50$  km depth) earthquakes. Next, after applying a Hanning taper, we compute the spectrum for a 12.8-second-long signal window beginning two seconds before each predicted arrival time and for a 12.8-second-long noise window just preceding this. We select spectra that have average signal-to-noise ratios of two or greater between 0.16 and 0.86 Hz. This results in 18,018  $P$  and 14,287  $PP$  spectra from 1553 events and 151 stations.

Each computed spectrum,  $D(f)$ , represents the effects of the source  $S(f)$ , attenuation  $A(f)$  and instrument  $R(f)$  responses:

$$D(f) = S(f)A(f)R(f)$$

We correct each spectrum for the known instrument response, an  $\omega^{-2.15}$  source model (found by Warren and Shearer, 2000, to be appropriate for this data set), and the globally-averaged  $Q$  model of Warren and Shearer (2000).

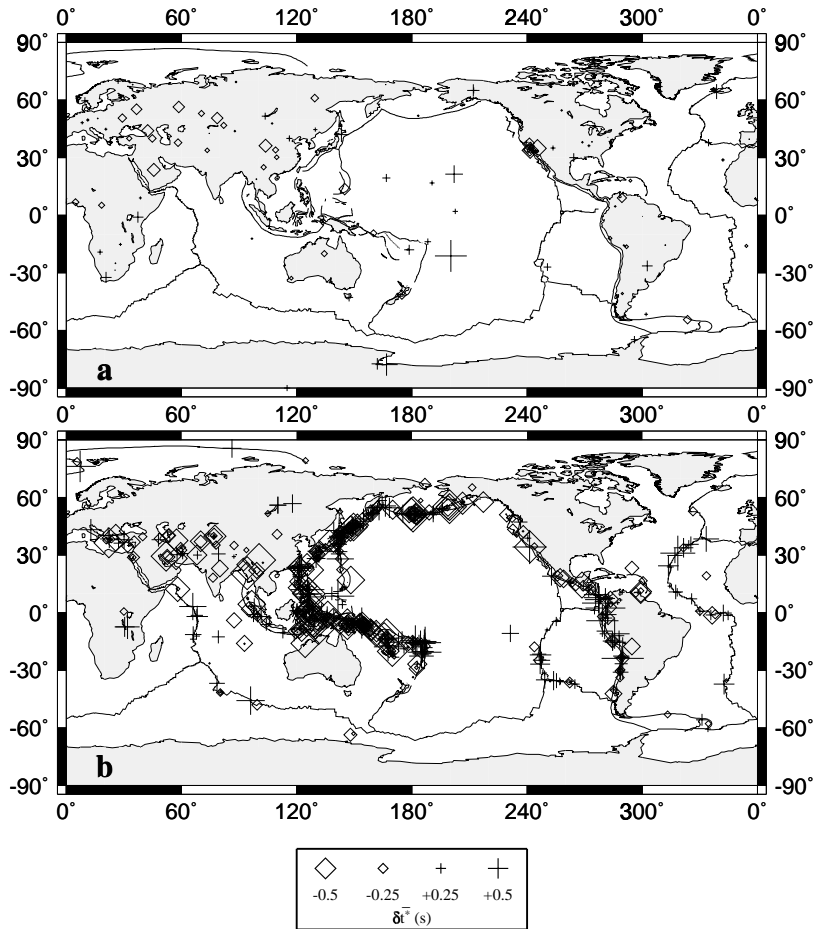


**Figure 1.** Residual  $\bar{t}^*$  measurements for stations (top) and events (bottom)

After these corrections are applied, the remaining spectrum represents deviations from the average attenuation response. The slope of the spectrum allows us to measure how much the wave has decayed along its path. The amplitude decay with frequency is given by  $A(f) = A_0 \exp(-\pi f t^*)$  where  $t^* = \int dt/Q$ . The apparent  $t^*$ , termed  $\bar{t}^*$ , can be measured by fitting a straight line to the spectrum in linear frequency - logarithmic amplitude space:

$$\bar{t}^* = t^* + f \frac{dt^*}{df} = -\frac{1}{\pi} \frac{d(\ln A)}{df}$$

When we measure residual  $\bar{t}^*$  (which we will refer as  $\delta\bar{t}^*$ ) from the spectrum, positive values indicate that a path is more attenuating than the average while negative values indicate that a path is less attenuating.

#### *Station and Source Terms*

We can measure the attenuation beneath each source and receiver by stacking the appropriate  $P$  spectra since we have multiple sources for each receiver and multiple receivers for each source. The resulting source-specific response functions include any remaining source spectrum and the effect of near-source attenuation in the upper mantle. The receiver stacks include the site response and near-receiver attenuation in the upper mantle. We measure  $\delta\bar{t}^*$  from the slope of the stacked spectra between 0.16 and 0.86 Hz. Maps showing the source and station terms are plotted in Figure 1 and show some coherent patterns. For example, the station and source  $\delta\bar{t}^*$  values across Eurasia are mostly negative, indicating that they are on less attenuating material. The variations we see, while relatively small in this region, are probably due to site effects and differences between sources. In other regions, there are much larger variations in  $\delta\bar{t}^*$  over relatively small areas.

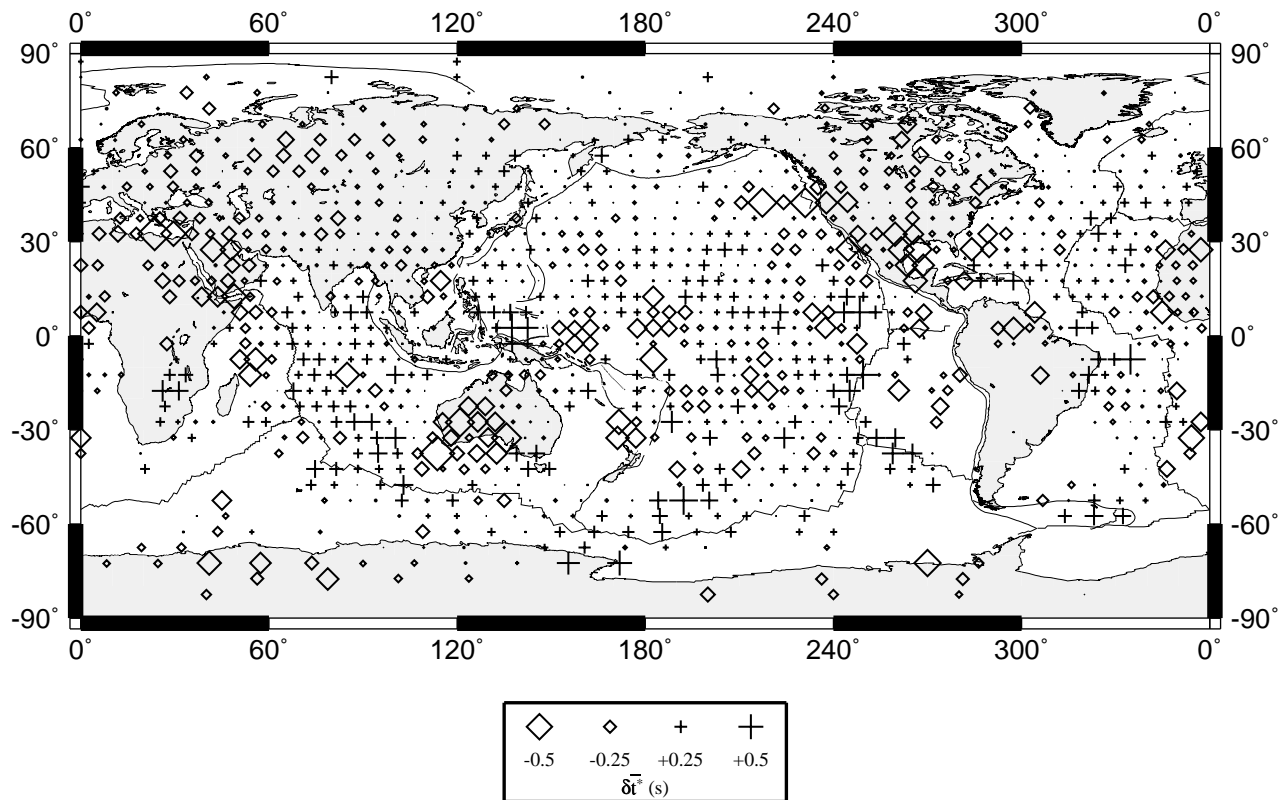


**Figure 2.** Residual  $\bar{t}^*$  measurements averaged in caps of  $5^\circ$  radius at the  $PP$  bouncepoints. There are a minimum of 5 measurements in each cap.

#### *Lateral Variations in $\bar{t}^*$*

While our station and source terms provide us with a preview of the lateral variations in upper mantle attenuation, they also reveal that they could be biased by local crustal structures or source differences. Since the  $PP$  spectra will be similarly affected, we correct them for the station and source terms. These terms include the propagation response in the upper mantle beneath the stations and earthquakes, so only attenuation accumulated along the rest of the  $PP$  path will be left in the spectrum. Since lower-mantle attenuation is small, the remaining spectrum should approximate attenuation near the  $PP$  bouncepoint in the upper mantle. We measure  $\delta \bar{t}^*$  between 0.16 and 0.86 Hz from the remaining spectrum. Since the individual  $\delta \bar{t}^*$  measurements exhibit considerable scatter, we smooth our results by computing the average values within  $PP$  bouncepoint caps of  $5^\circ$  radius spaced by  $5^\circ$ . The cap-averaged results are plotted in Figure 2. Larger symbols indicate larger-magnitude variations.

Our results are in general agreement with previous upper mantle  $Q$  models (e.g., Romanowicz, 1995; Bhattacharyya et al., 1996). The shields across Eurasia and North America are less attenuating (negative  $\delta \bar{t}^*$  values) while more attenuating regions (positive  $\delta \bar{t}^*$  values) are found along the mid-ocean-ridge system and in the mid-Pacific. These patterns suggest that the amount of attenuation correlates with the tectonic setting. Indeed, when we bin the caps by tectonic region (following Jordan, 1981) and compute the mean value for each type of region (Figure 3) we see that the mean values follow a pattern consistent with that expected based on their tectonic history. The upper mantle beneath young ocean floor, where hot material is upwelling, is the most attenuating type of region, followed closely by intermediate-age oceans. Old oceans are much less attenuating than young oceans. The least attenuating regions are the old shields and platforms. There are exceptions to these patterns. For example, beneath southern Africa we see a more attenuating region and in the southwest Pacific we see a less attenuating region.

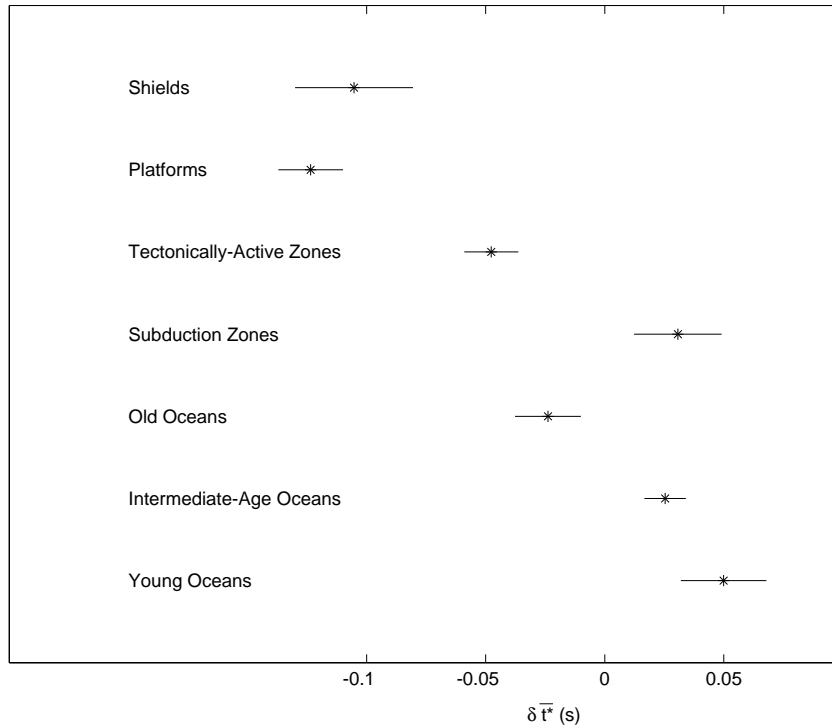


**Figure 3.** Average residual  $\bar{t}^*$  measurements plotted for  $PP$  bouncepoints in different tectonic regions. One-standard-error bars are also shown.

## CONCLUSIONS AND RECOMMENDATIONS

Variations in upper mantle  $Q_\alpha$  can be mapped by analyzing global data sets of short-period  $P$  and  $PP$  spectra. Given sufficient data, the effects of variations in source spectra and receiver site response can be removed, permitting along-path attenuation to be resolved. Our results are generally consistent with previous studies which show a correlation of upper mantle attenuation structure with tectonic region. Continued research will help to calibrate magnitude versus yield relationships over large parts of the Earth's surface.

## REFERENCES

- Bhattacharyya, J., G. Masters, and P.M. Shearer, Global lateral variations of shear wave attenuation in the upper mantle, *J. Geophys. Res.*, 101, 22,273–22,289, 1996.
- Jordan, T.H., Global tectonic regionalization for seismological data analysis, *Bull. Seismol. Soc. Am.*, 71, 1131–1141, 1981.
- Romanowicz, B., A global tomographic model of shear attenuation in the upper mantle, *J. Geophys. Res.*, 100, 12,375–12,394, 1995.
- Warren, L.M., and P.M. Shearer, Investigating the frequency dependence of mantle  $Q$  by stacking  $P$  and  $PP$  spectra, *J. Geophys. Res.*, submitted 2000.